ORIGINAL ARTICLE

MicrobiologyOpen WILEY

Spo0J and SMC are required for normal chromosome segregation in *Staphylococcus aureus*

Helena Chan 🆔 | Bill Söderström | Ulf Skoglund

Structural Cellular Biology Unit, Okinawa Institute of Science and Technology, Okinawa, Japan

Correspondence
Helena Chan, The ithree institute, University of Technology Sydney, Broadway, NSW, Australia.
Email: helenayee-wah.chan@uts.edu.au

Present address
Helena Chan and Bill Söderström, The ithree institute, University of Technology Sydney, Broadway, NSW, Australia

Abstract

Bacterial chromosome segregation is an essential cellular process that is particularly elusive in spherical bacteria such as the opportunistic human pathogen *Staphylococcus aureus*. In this study, we examined the functional significance of a ParB homologue, Spo0J, in staphylococcal chromosome segregation and investigated the role of the structural maintenance of chromosomes (SMC) bacterial condensin in this process. We show that neither *spo0J* nor *smc* is essential in *S. aureus*; however, their absence causes abnormal chromosome segregation. We demonstrate that formation of complexes containing Spo0J and SMC is required for efficient *S. aureus* chromosome segregation and that SMC localization is dependent on Spo0J. Furthermore, we found that cell division and cell cycle progression are unaffected by the absence of *spo0J* or *smc*. Our results verify the role of Spo0J and SMC in ensuring accurate staphylococcal chromosome segregation and also imply functional redundancy or the involvement of additional mechanisms that might contribute to faithful chromosome inheritance.

KEYWORDS

cell division, chromosome segregation, condensin complexes, DNA-binding proteins, microscopy, *Staphylococcus aureus*

1 | INTRODUCTION

Staphylococcus aureus is a Gram-positive, spherical bacterium that divides in three consecutive, orthogonal planes (Monteiro et al., 2015; Pinho, Kjos, & Veening, 2013; Tzagoloff & Novick, 1977). As is the case for all bacteria, replicated chromosomes must be efficiently segregated to ensure accurate inheritance of genetic material (Badrinarayanan, Le, & Laub, 2015; Bloom & Joglekar, 2010; Graumann, 2014; Toro & Shapiro, 2010; Wang, Llopis, & Rudner, 2013). How this is achieved in dividing *S. aureus* cells is still poorly understood.

The prototypical DNA segregation system, *parABS*, was first identified and studied on prophage and *Escherichia coli* plasmids (Baxter & Funnell, 2014; Gerdes, Howard, & Szardenings, 2010; Hayes &

Barilla, 2006; Oliva, 2016; Salje, 2010; Schumacher, 2012), however, homologues are also present on most bacterial chromosomes (Livny, Yamaichi, & Waldor, 2007). The *parABS* system consists of a Walker-type ATPase (ParA/Soj), a DNA-binding protein (ParB/Spo0J), and repetitive centromere-like sequences (*parS*) (Baxter & Funnell, 2014; Gerdes et al., 2010; Salje, 2010). Generally, ParB proteins bind specifically to *parS* sites that are located in the origin-proximal region to form a nucleoprotein complex (Breier & Grossman, 2007; Lin & Grossman, 1998; Minnen, Attaiech, Thon, Gruber, & Veening, 2011; Murray, Ferreira, & Errington, 2006). ParA proteins bind nonspecifically to nucleoid DNA and interact with *parS*-bound ParB proteins (Lutkenhaus, 2012; Vecchiarelli, Hwang, & Mizuuchi, 2013; Vecchiarelli, Neuman, & Mizuuchi, 2014). Recently, it was found that ParB binds cytidine triphosphate (CTP) and exhibits *parS*-dependent CTP hydrolysis to

modulate *parS* binding and recruitment of ParA (Osorio-Valeriano et al., 2019; Soh et al., 2019). Interaction with ParB stimulates the ATPase activity of ParA and releases ParA from the ParB/*parS* complex, ultimately creating a gradient of ParA that drives DNA segregation toward the cell poles (Hatano & Niki, 2010; Sanchez, Rech, Gasc, & Bouet, 2013; Vecchiarelli et al., 2014).

An *S. aureus* Spo0J homologue exhibits 47% identity with *Bacillus subtilis* Spo0J. However, similar to *Streptococcus pneumoniae*, *S. aureus* does not encode a ParA/Soj homologue, suggesting that the mechanism of chromosome segregation in *S. aureus* may deviate from canonical mechanisms described thus far.

Studies in *S. pneumoniae* and *B. subtilis* show that the structural maintenance of chromosomes (SMC) protein is recruited to origin-proximal sites through interaction with ParB/Spo0J (Gruber & Errington, 2009; Minnen et al., 2011; Sullivan, Marquis, & Rudner, 2009). SMC (MukB in *E. coli*) is a condensin that, in complex with ScpA and ScpB, contributes to chromosome compaction and organization (Britton, Lin, & Grossman, 1998; Mascarenhas, Soppa, Strunnikov, & Graumann, 2002; Moriya et al., 1998; Wang, Tang, Riley, & Rudner, 2014). In the absence of both *B. subtilis* Spo0J and SMC, chromosome segregation defects are amplified compared to the absence of either gene alone, suggesting a role for Spo0J and SMC interaction in chromosome segregation (Britton et al., 1998; Lee & Grossman, 2006; Wang et al., 2014). A previous study has shown that SMC also contributes to staphylococcal chromosome segregation, since a significant proportion of cells lacking SMC were anucleate (Yu, Herbert, Graumann, & Götz, 2010). However, little is known about the functional significance of *S. aureus* Spo0J and its interactions, if any, with SMC.

Based on the function of ParB/Spo0J proteins, we sought to verify the role of Spo0J in staphylococcal chromosome segregation and its potential role in SMC function. We used super-resolution structured illumination microscopy (SIM) to confirm that Spo0J is indeed involved in *S. aureus* chromosome segregation, but found that it is not essential for growth and viability. We also show that Spo0J is required for correct localization of SMC and that both proteins act in concert to ensure efficient chromosome segregation, however, a role in cell division was not immediately evident. Our data indicate the involvement of additional interactions that influence *S. aureus* chromosome segregation and cell division, suggesting redundancy or overlapping roles of proteins involved in these essential processes.

2 | MATERIALS AND METHODS

2.1 | Bacterial strains and growth

Bacterial strains used in this study are listed in Table 1. Molecular cloning and plasmid propagation were performed using *E. coli* DC10B cells grown in Luria-Bertani (LB) broth (Sigma-Aldrich). *Staphylococcus aureus* RN4220 strains were grown in tryptic soy broth (TSB; Becton Dickinson Bacto™), minimal media (SSM9PR: 1 × M9 salts [6.8 g/L Na_2HPO_4, 3 g/L KH_2PO_4, 0.5 g/L NaCl, 1 g/L

NH_4Cl], 2 mM $MgSO_4$, 0.1 mM $CaCl_2$, 1% (w/v) glucose, 1% (w/v) casamino acids, 1.5 µM thiamine, 0.05 mM nicotinamide), or on brain heart infusion (BHI) agar (Becton Dickinson Difco™). Liquid cultures were routinely grown at 37°C with aeration, unless otherwise specified.

Plasmids were introduced into chemically competent *E. coli* DC10B or BTH101 cells using heat shock (Sambrook & Russell, 2001). Plasmids isolated from *E. coli* DC10B strains were introduced into *S. aureus* RN4220 cells via electroporation (Löfblom, Kronqvist, Uhlén, Ståhl, & Wernérus, 2007; Monk, Shah, Xu, Tan, & Foster, 2012). Where applicable, antibiotics were used at the following concentrations: 100 µg/ml ampicillin, 50 µg/ml kanamycin, 10 µg/ml erythromycin, and 15 µg/ml neomycin. Details on the construction of strains used in this study are provided in Appendix 1.

2.2 | Recombinant DNA techniques

Plasmids used in this study are listed in Table 1. Oligonucleotides were synthesized by Integrated DNA Technologies and are listed in Table A1. DNA modification enzymes were purchased from New England Biolabs.

Plasmids were constructed using standard molecular cloning techniques (Sambrook & Russell, 2001) with T4 DNA ligase or Gibson assembly (Gibson et al., 2009) using Q5 high-fidelity DNA polymerase, T5 exonuclease, and Taq DNA ligase. Plasmid DNA was isolated from *E. coli* DC10B cells using the QIAprep Spin Miniprep kit (Qiagen). *Staphylococcus aureus* genomic DNA was isolated using the Purelink Genomic DNA Mini kit (Invitrogen), with the addition of 50 µg/ml lysostaphin (Sigma-Aldrich) for cell lysis at 37°C for 30 min. DNA purification was performed using the NucleoSpin Gel and PCR Clean-up kit (Macherey-Nagel). Details on the construction of plasmids used in this study are provided in Appendix 1. Plasmid sequences were verified by DNA sequencing (Fasmac).

2.3 | Bacterial growth assays

Overnight cultures of strains to be assayed were diluted 1:50 in fresh media (SSM9PR minimal media or TSB rich media) and grown at 37°C until OD_{600nm} ~ 0.05. Cultures were aliquoted in triplicate into separate wells of a 96-well microplate. Optical density was measured every 20 min at 595 nm using a MultiSkan Go microplate reader (Thermo Fisher Scientific) set at 37°C with moderate shaking. Experiments were performed in triplicate for at least three independent experiments.

2.4 | Bacterial viability assays

Overnight cultures were diluted 1:50 in fresh media and grown to mid-exponential phase. Cultures were normalized to OD_{600nm} 1.0

TABLE 1 Bacterial strains and plasmids used in this study

Strain or plasmid	Relevant genotype or description	Reference
Escherichia coli		
DC10B	*E. coli* K-12 (DH10B) derivative. $\Delta dcm\ dam^+\ \Delta hsdRMS\ endA1\ recA1$	Monk et al. (2012)
BTH101	F^-, *cya-99, araD139, galE15, galK16, rpsL1 (Str^r), hsdR2, mcrA1, mcrB1*	Karimova et al. (1998)
Staphylococcus aureus		
RN4220	Restrictionless derivative of NCTC 8325–4	Kreiswirth et al. (1983)
HC061	RN4220 $\Delta spo0J$	This study
HC080	RN4220 Δsmc	This study
HC094	RN4220 $\Delta spo0J\ \Delta smc$	This study
Plasmids		
pHC052	pSK1 *ori*, Amp^R, Neo^R, P$_{xyl/tetO}$-*spo0J-mRFPmars*	This study
pHC061	pMAD containing *S. aureus* RN4220 *spo0J* upstream and downstream regions, Amp^R, Ery^R	This study
pHC067	pSK41 *ori*, Amp^R, Ery^R, P$_{spac}$-*smc-gfp*	This study
pHC080	pMAD containing *S. aureus* RN4220 *smc* upstream and downstream regions, Amp^R, Ery^R	This study
pHC102	pSK41 *ori*, Amp^R, Ery^R, P$_{spac}$-*gfp*	This study
pHC111	pKNT25 derivative encoding Spo0J-T25, Kan^R, P$_{lac}$-*spo0J-T25*	This study
pHC112	pKNT25 derivative encoding SMC-T25, Kan^R, P$_{lac}$-*smc-T25*	This study
pHC114	pUT18 derivative encoding Spo0J-T18, Amp^R, P$_{lac}$-*spo0J-T18*	This study
pHC115	pUT18 derivative encoding SMC-T18, Amp^R, P$_{lac}$-*smc-T18*	This study
pKNT25	Encodes T25 fragment (residues 1–224) of adenylate cyclase, CyaA, fused in frame downstream of MCS, Kan^R	Karimova et al. (1998)
pKT25-zip	pKT25 derivative encoding the leucine zipper of GCN4, Kan^R, P$_{lac}$-*T25-zip*	Euromedex
pUT18	Encodes T18 fragment (residues 225–399) of adenylate cyclase, CyaA, fused in frame downstream of MCS, Amp^R	Karimova et al. (1998)
pUT18C-zip	pUT18C derivative encoding the leucine zipper of GCN4, Amp^R, P$_{lac}$- *T18-zip*	Euromedex
pMAD	Allelic replacement vector; pBR322 and pE194ts origins of replication in *E. coli* and staphylococci, Amp^R, Ery^R	Arnaud, Chastanet, and Débarbouillé (2004)
pSK9065	*E. coli–S. aureus* shuttle vector carrying low-copy number *S. aureus* pSK1 origin of replication and anhydrotetracycline-inducible P$_{xyl/tetO}$ promoter, Amp^R, Neo^R	Brzoska and Firth (2013)
pSK9067	*E. coli–S. aureus* shuttle vector carrying low-copy number *S. aureus* pSK41 origin of replication and IPTG-inducible P$_{spac}$ promoter and optimized lacO$_{id}$ operator, Amp^R, Ery^R	Brzoska and Firth (2013)

Note: Amp^R, confers ampicillin resistance; Ery^R, confers erythromycin resistance; Kan^R, confers kanamycin resistance; Neo^R, confers neomycin resistance; *ori*, origin of replication.

and serially diluted in phosphate-buffered saline (PBS), after which 10 μl was spotted onto SSM9PR minimal media agar or BHI agar plates. Plates were incubated overnight at 37°C. Data were obtained from at least three independent experiments.

2.5 | Bacterial two-hybrid assays

Escherichia coli adenylate cyclase, *cya*, mutant cells (BTH101) were cotransformed with pairs of pKNT25 and pUT18 plasmid derivatives. Five single colonies of each strain were patched onto selective LB agar plates containing 100 μg/ml 5-bromo-4-chloro-3-indolyl-β-D-galactopyranoside (X-Gal; Sigma-Aldrich) and 0.5 mM isopropyl β-D-1-thiogalactopyranoside (IPTG; Sigma-Aldrich). Plates were

incubated at 30°C for 3 days. Blue patches indicate β-galactosidase activity from interaction between T25 and T18 fusions. Data shown are representative of three independent assays.

2.6 | Fluorescence microscopy

Overnight cultures of *S. aureus* cells were diluted 1:50 in fresh TSB with appropriate antibiotics and incubated at 37°C with aeration until mid-exponential phase (OD$_{600nm}$ ~ 0.4–0.6). For fluorescence localization of Spo0J-mRFPmars and SMC-GFP, cultures were grown at 30°C until OD$_{600nm}$ ~ 0.1–0.2. Expression of Spo0J-mRFPmars and SMC-GFP was induced for 2 hr with 2.5 ng/ml anhydrotetracycline and 0.1 mM IPTG, respectively. Where required, DNA was

stained with 2.5 μg/ml 4′,6-diamidino-2-phenylindole (DAPI), cell membranes were stained with 5 μg/ml FM4-64 (Invitrogen), and cell walls were stained with an equal mixture of vancomycin and a vancomycin BODIPY FL conjugate (0.4 μg/ml, Invitrogen) for 2 min at room temperature. After washing with PBS, a small aliquot of cells was applied to an agarose pad containing 2% (w/v) agarose in TSB on a microscope slide, and then covered with a glass coverslip for imaging.

Super-resolution SIM imaging was performed using a Zeiss ELYRA PS.1 microscope equipped with a 100 × 1.46 NA alpha plan apochromat oil immersion objective and a pco.edge sCMOS camera. Fluorescence images were acquired sequentially using 200–300 ms exposure times per image, for a total of 15 images per SIM reconstruction. All imaging was performed at room temperature (~23°C). Raw data were reconstructed using the SIM algorithms in ZEN 2011 SP7 software (black edition, Carl Zeiss). Brightfield images were captured using widefield imaging mode. Images had a final pixel size of 25 nm × 25 nm.

Images were processed and analyzed using Fiji (Schindelin et al., 2012). Cell diameters were determined by measuring the distance between FM4-64 fluorescence peaks from line profiles drawn along the short axis of cells. Data were obtained from at least three independent experiments.

2.7 | Western blot and immunodetection

Staphylococcus aureus cultures were grown using the growth and induction conditions described for fluorescence microscopy. Following induction for 2 hr, cells were harvested (1,800 *g*, 4°C, 10 min) and then resuspended 1:200 in lysis buffer (0.1 M NaCl, 0.1 M Tris-HCl, 0.01 M MgCl$_2$, pH 7.5) containing 1 × protease inhibitor cocktail (Roche) and 0.1 mg/ml DNaseI (Roche). Cells were mixed with 212–300 μm acid-washed glass beads (Sigma-Aldrich) and lysed at 50 Hz for 6 min using a TissueLyser (Qiagen) with precooled tube adapter. Lysates were cleared by centrifugation (21,100 *g*, 4°C, 30 min) and then incubated with reducing sample buffer at 95°C for 5 min. Samples were electrophoresed on 4%–15% Tris-glycine polyacrylamide gradient gels and then transferred to 0.45 μm nitrocellulose membranes in Towbin buffer (25 mM Tris, 192 mM glycine, 20% (v/v) methanol, pH 8.3).

Blots were blocked with 5% (w/v) EasyBlocker (GeneTex) in TBST (25 mM Tris, 0.15 M NaCl, 0.05% Tween-20). Spo0J-mRFPmars was detected with a 1:2,000 dilution of anti-RFP or anti-mCherry antibodies (Abcam), and SMC-GFP and GFP were detected with a 1:3,000 dilution of anti-GFP antibodies (Abcam). Primary antibodies were detected with a 1:3,000 dilution of goat anti-rabbit HRP-conjugated antibodies (Bio-Rad). Antibodies were diluted in blocking buffer and incubated with blots for 1 hr at room temperature. Blots were washed three times with TSBT before and after blocking and antibody incubations. Secondary antibodies were detected using Clarity Western ECL substrate (Bio-Rad). Blots were imaged using a ChemiDoc gel imager (Bio-Rad).

2.8 | Immunoprecipitation

Immunoprecipitation experiments were performed on *S. aureus* cell lysates prepared as described for Western blotting. Cell lysates (~1.5 mg total protein) from *S. aureus* cells expressing Spo0J-mRFPmars (pHC052) and either GFP (pHC102) or SMC-GFP (pHC067) were incubated with pre-equilibrated GFP-Trap magnetic agarose beads (ChromoTek) for 1 hr at 4°C with gentle inversion. Beads were magnetically separated and washed twice with wash buffer (10 mM Tris-HCl, 150 mM NaCl, 0.5 mM EDTA, pH 7.5) at 4°C, before elution of bound complexes with elution buffer (50 mM Tris-HCl, 10 mM EDTA, 1% SDS, pH 8) at 65°C for 15 min. Eluates were magnetically separated from the beads and analyzed by Western blotting and immunodetection.

2.9 | Statistical analyses

Analyses of statistical significance were performed using unpaired Student's *t* tests. *p* values <.05 were considered statistically significant and are indicated with asterisks.

3 | RESULTS

3.1 | *spo0J* and *smc* are not essential for *Staphylococcus aureus* growth and viability

There is much variation in the functional significance of ParB and SMC in different bacteria. For example, *parB* is essential in *Caulobacter crescentus*, while its homologue *spo0J* is not essential in *B. subtilis* nor *S. pneumoniae* (Ireton, Gunther, & Grossman, 1994; Minnen et al., 2011; Mohl, Easter, & Gober, 2001). Additionally, *smc* is not essential in *S. pneumoniae* and *C. crescentus*, but deletion causes lethality under conditions promoting fast growth in *B. subtilis* (Gruber et al., 2014; Jensen & Shapiro, 1999; Minnen et al., 2011). In order to determine whether *spo0J* and *smc* are essential in *S. aureus*, we generated separate *spo0J* and *smc* deletions in the *S. aureus* RN4220 parental strain. Strains were constructed using an integrative pMAD derivative followed by double-crossover homologous recombination to generate markerless deletions at the *spo0J* or *smc* loci of the *S. aureus* RN4220 genome (Appendix 1). Furthermore, because *spo0J* and *smc* were shown to interact in *B. subtilis* and *S. pneumoniae*, we also constructed a Δ*spo0J* Δ*smc* double mutant to test whether this interaction is essential in *S. aureus*.

The Δ*spo0J* (HC061), Δ*smc* (HC080), and Δ*spo0J* Δ*smc* (HC094) mutants showed similar growth rates to the RN4220 parental strain, with no difference in viability when grown at 37°C in TSB rich medium or SSM9PR minimal medium (Figure 1a–c). As described below, we showed that the lack of significant difference in growth and viability between the strains was not a result of suppressor mutations or polar effects from the gene deletions (Figure A1).
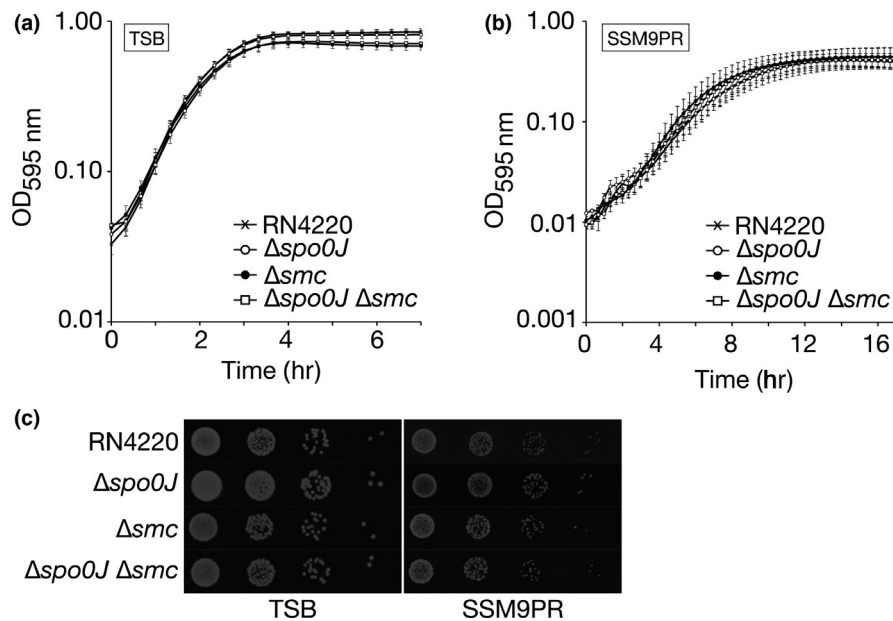
FIGURE 1 Growth and viability of *Staphylococcus aureus* cells in the absence of Spo0J and SMC. Growth of *S. aureus* parental strain (RN4220) (cross), Δ*spo0J* (open circle), Δ*smc* (closed circle), and Δ*spo0J* Δ*smc* (open square) at 37°C in rich TSB (a) or SSM9PR minimal media (b) was monitored by measuring the optical density at 595 nm every 20 min. (c) Viability assays of RN4220, Δ*spo0J*, Δ*smc*, and Δ*spo0J* Δ*smc* at 37°C in TSB (left) and SSM9PR (right) media. Mid-exponential phase cultures were normalized to OD_{600nm} 1.0, then serially diluted in PBS and spotted onto the respective agar plates. Dilutions from left to right: 10^{-3}, 10^{-4}, 10^{-5}, and 10^{-6}. Data are representative of three independent experiments

3.2 | Spo0J and SMC are involved in *Staphylococcus aureus* chromosome segregation

The roles of Spo0J and SMC in chromosome segregation are well-studied in *B. subtilis* and *S. pneumoniae*. Perturbations to *spo0J* or *smc* result in defects in chromosome segregation, with a *spo0J smc* double mutant having a synthetic lethal phenotype in *B. subtilis* when grown in rich medium (Britton et al., 1998). Yu et al. (2010) showed that SMC is involved in *S. aureus* chromosome segregation, but we wondered whether *spo0J* also plays a role together with SMC. To this end, we performed SIM imaging to examine the DNA content of *S. aureus* RN4220, Δ*spo0J*, Δ*smc*, and Δ*spo0J* Δ*smc* derivatives stained with DAPI.

When grown at 37°C in TSB rich medium, 0.1% of the RN4220 parental strain contained cells that were anucleate, that is, without a nucleoid and, therefore, devoid of DAPI staining (Figure 2a,b). In comparison, 0.6% of Δ*spo0J* and 1.1% of Δ*smc* cells were anucleate, which are both significantly greater than the frequency observed for the parental strain (p = .0241 and 0.0021, respectively) (Figure 2a,b), suggesting that *spo0J* and *smc* are required for normal chromosome segregation in *S. aureus*. Notably, the Δ*spo0J* Δ*smc* double mutant showed a significantly higher proportion of anucleate cells compared to the parental strain and the Δ*spo0J* and Δ*smc* single mutants (3.2% anucleate cells, p = .0017, 0.0032, and 0.0070, respectively) (Figure 2a,b), indicating an increased chromosome segregation defect in the absence of both *spo0J* and *smc*.

Defects in chromosome segregation are often associated with nucleoid abnormalities such as nucleoid condensation or bisection

of unsegregated nucleoids by the division septum (Minnen et al., 2011; Veiga & G Pinho, 2017; Yu et al., 2010). However, in our study, we found no difference in the occurrence of nucleoid abnormalities between the parental and mutant strains and did not observe any instances of septum formation over unsegregated chromosomes.

3.3 | Spo0J is required for SMC localization in *Staphylococcus aureus*

Our finding that Spo0J and SMC are both required together to ensure accurate chromosome segregation led us to speculate that *S. aureus* Spo0J and SMC might behave similarly to their counterparts in other bacteria. A significant role of ParB/Spo0J in *S. pneumoniae*, *B. subtilis*, and *C. crescentus* is to recruit the condensin, SMC, to origin-proximal sites, where ParB/Spo0J binds (Gruber & Errington, 2009; Minnen et al., 2011; Sullivan et al., 2009; Tran, Laub, & Le, 2017). To determine whether this interaction might also occur in *S. aureus*, we constructed Spo0J-mRFPmars and SMC-GFP fusion proteins so that their localizations could be visualized by SIM imaging. Both proteins were expressed from compatible, coresident, low-copy number plasmids in *S. aureus*. Spo0J-mRFPmars expression was induced with 2.5 ng/ml anhydrotetracycline from the $P_{xyl/tetO}$ promoter, while SMC-GFP expression was induced with 0.1 mM IPTG from the P_{spac} promoter. Importantly, both fluorescent fusions were functional under the induction conditions tested, since Spo0J-mRFPmars and SMC-GFP could complement the chromosome segregation defects
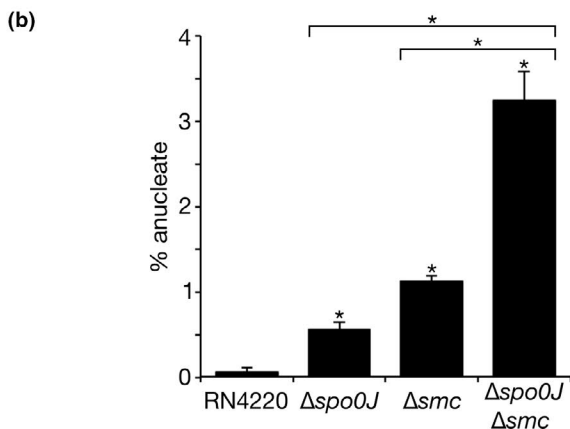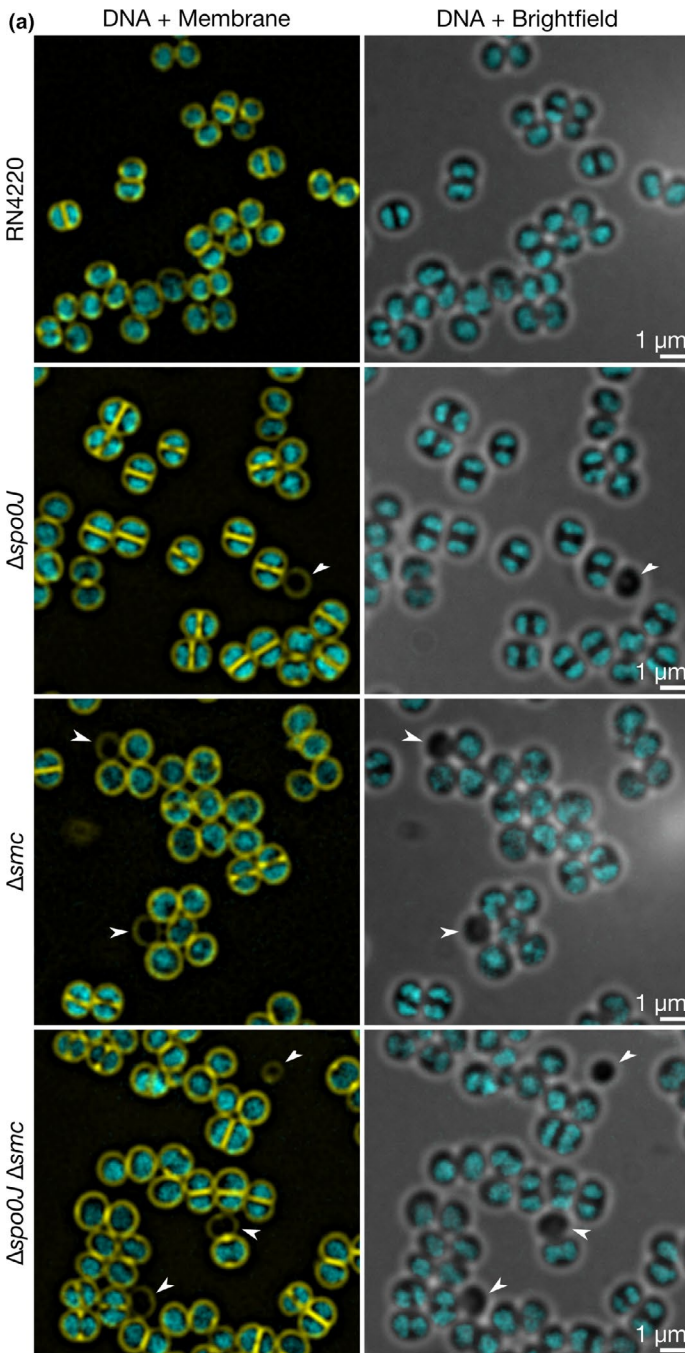
FIGURE 2 Chromosome segregation in *Staphylococcus aureus* cells lacking Spo0J and SMC. (a) Super-resolution SIM images of mid-exponential phase *S. aureus* parental (RN4220), Δ*spo0J*, Δ*smc*, and Δ*spo0J* Δ*smc* strains. Cell membranes (yellow) were stained with the lipid dye FM4-64. DNA (cyan) was stained with DAPI. Left: merge of cell membrane and DNA fluorescence. Right: merge of DNA fluorescence and brightfield images. Arrowheads indicate anucleate cells. Scale bars = 1 μm. (b) Frequency of anucleate cells in the presence and absence of *spo0J* and *smc*, calculated from SIM fluorescence micrographs. Data represent averages of three independent experiments. n_{total} = 1,233, 2,552, 2,075, and 2,846 cells for RN4220, Δ*spo0J*, Δ*smc* and Δ*spo0J* Δ*smc* strains, respectively. Error bars indicate standard error of the mean. *$p < .05$, considered statistically significant (unpaired Student's *t* test)
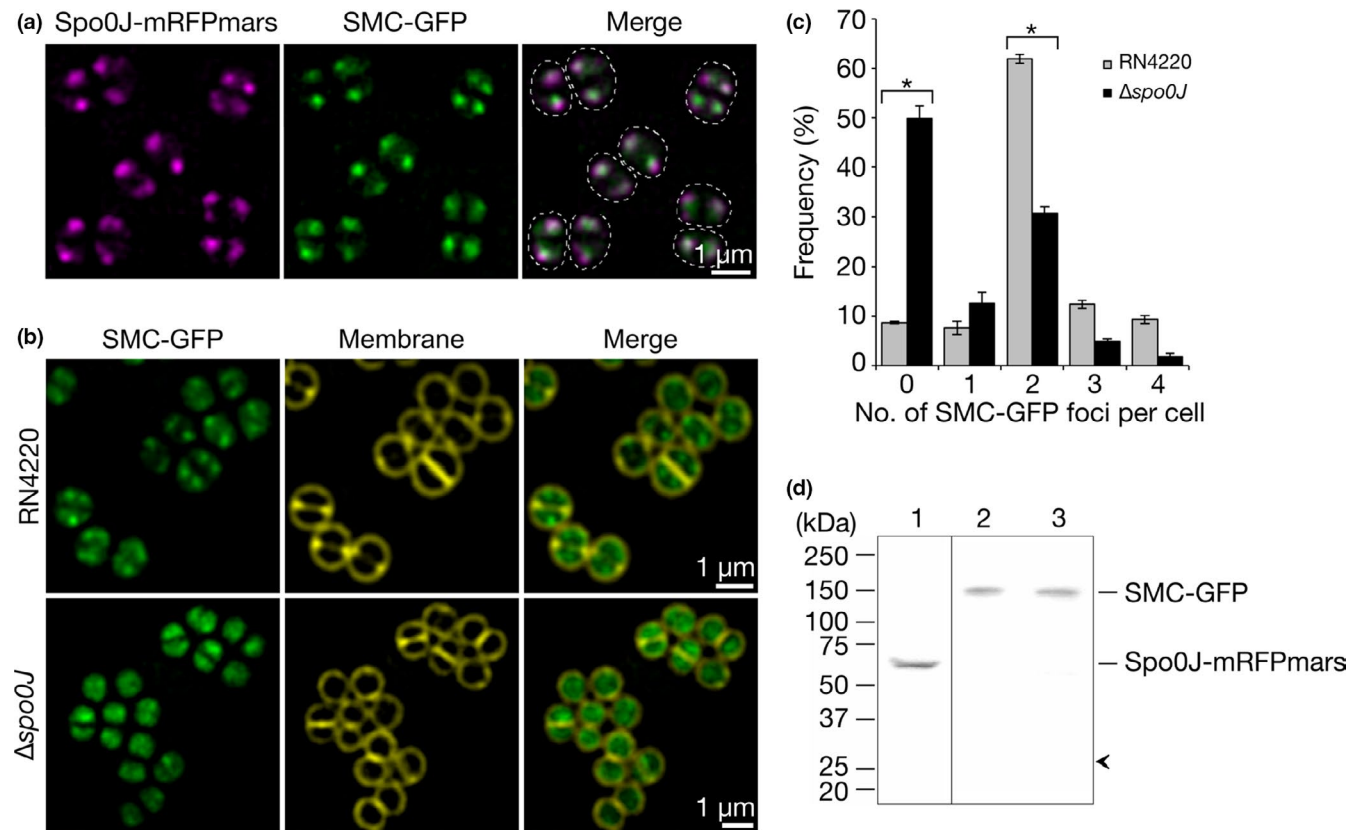
FIGURE 3 SMC localization requires Spo0J. (a) SIM images showing dual fluorescence localization of Spo0J-mRFPmars (magenta) and SMC-GFP (green) in *Staphylococcus aureus* RN4220. Cell outlines are indicated with white dashed lines. Scale bar = 1 μm. (b) SIM images of mid-exponential phase *S. aureus* cells expressing SMC-GFP (green) in the presence (RN4220) and absence (Δ*spo0J*) of *spo0J*. Cell membranes (yellow) were stained with the lipid dye FM4-64. Scale bars = 1 μm. (c) Frequency of fluorescent SMC-GFP foci in RN4220 and Δ*spo0J* cells. Data represent averages of three independent experiments. n_{total} = 1,307 and 1,345 cells for RN4220 and Δ*spo0J* strains, respectively. Error bars indicate standard error of the mean. *$p < .0001$, considered statistically significant (unpaired Student's *t* test). (d) Western blot analysis of Spo0J-mRFPmars in *S. aureus* RN4220 (lane 1), SMC-GFP in *S. aureus* RN4220 (lane 2), and SMC-GFP in *S. aureus* RN4220 Δ*spo0J* (lane 3). Spo0J-mRFPmars and SMC-GFP were detected in *S. aureus* cell lysates using anti-mCherry and anti-GFP antibodies, respectively. Arrowhead indicates the predicted position of free mRFPmars or GFP (~27 kDa). No proteolysis of Spo0J-mRFPmars or SMC-GFP was observed

of the Δ*spo0J* and Δ*smc* mutants, respectively (Figure A1). This further verifies that the growth, viability, and chromosome segregation phenotypes of the Δ*spo0J* and Δ*smc* strains were the result of gene deletions and not other mutations or polar effects.

Spo0J-mRFPmars formed fluorescent foci consistent with previously shown localization patterns and indicative of DNA-binding to origin-proximal sites (Pinho & Errington, 2004; Veiga, Jorge, & Pinho, 2011) (Figure 3a and Figure A2). SMC-GFP displayed similar localization patterns to Spo0J-mRFPmars, often with overlapping, or partially-overlapping, foci (Figure 3a). Our results suggest that *S. aureus* Spo0J and SMC likely localize to similar subcellular positions, consistent with potential complex formation.

If *S. aureus* Spo0J recruits SMC to origin-proximal sites as described in *B. subtilis*, *S. pneumoniae*, and *C. crescentus* (Gruber & Errington, 2009; Minnen et al., 2011; Sullivan et al., 2009; Tran et al., 2017), then we predicted that SMC-GFP might be mis-localized in the absence of Spo0J. Therefore, we endeavored to determine whether SMC-GFP localization is dependent on Spo0J. For this

purpose, we expressed SMC-GFP in the *S. aureus* Δ*spo0J* mutant strain and compared its localization to that in the parental RN4220 strain. Subsequent SIM imaging revealed that more than 90% of cells in the parental strain contained at least one fluorescent focus of SMC-GFP, with the majority (62%) containing two SMC-GFP foci per cell (Figure 3b,c). In contrast, SMC-GFP localization appeared more dispersed in the Δ*spo0J* cells, with a significantly higher proportion of cells containing no SMC-GFP foci (50%, $p < .0001$), and an average of 0.96 foci per cell, compared to 2.1 foci in the parental strain ($p < .0001$, n_{total} = 1,345 and 1,307 cells, respectively, Figure 3b,c). Western blotting using anti-GFP antibodies showed that the loss of SMC-GFP foci in the absence of *spo0J* was not due to the release of free GFP by proteolysis (Figure 3d). No proteolysis was also detected for Spo0J-mRFPmars (Figure 3d). Taken together, our results suggest that staphylococcal chromosome segregation involves the formation of complexes containing Spo0J and SMC and that Spo0J is required for correct localization of SMC in *S. aureus*.
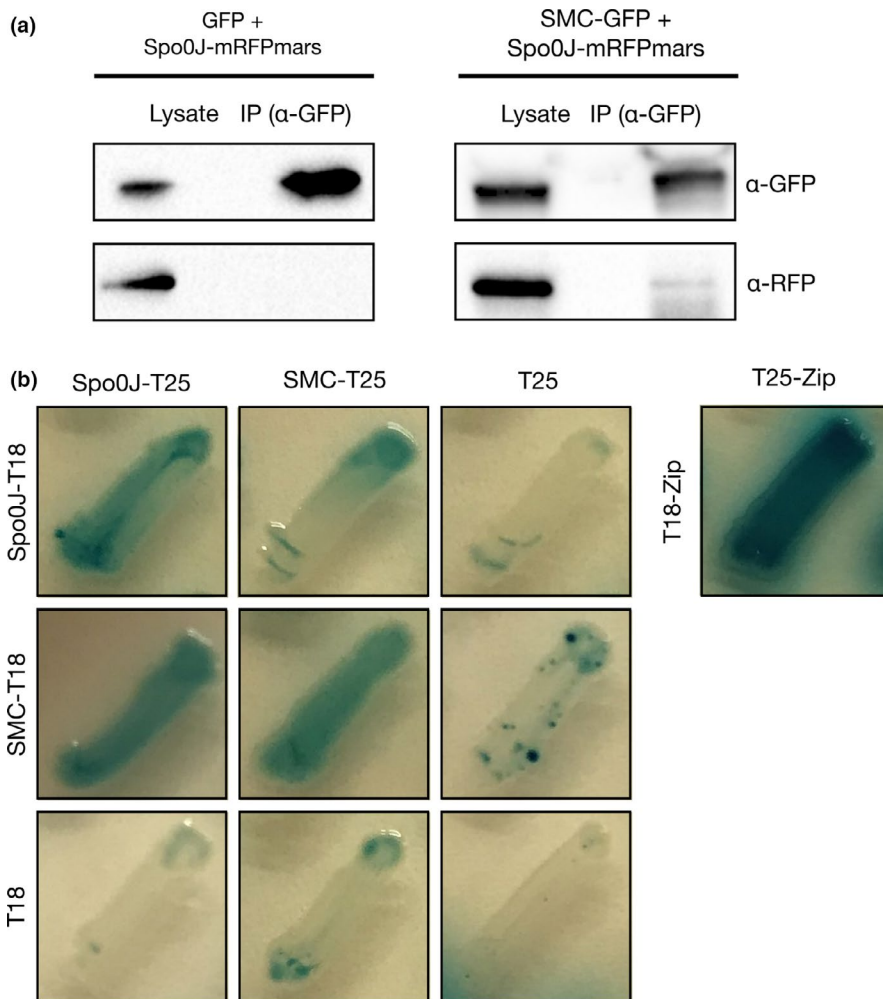
(a)

(b)

FIGURE 4 Interactions involving *Staphylococcus aureus* Spo0J and SMC. (a) Western blot analysis of immunoprecipitation from *S. aureus* cells expressing Spo0J-mRFPmars and either GFP or SMC-GFP. Proteins were immunoprecipitated using anti-GFP antibodies. Lysates and immunoprecipitated proteins were probed using anti-GFP and anti-RFP antibodies. Brightness of Spo0J-mRFPmars immunoblot (bottom panel) was increased to enhance visualization of the immunoprecipitated protein band. (b) Bacterial two-hybrid assay of Spo0J and SMC fused to *B. pertussis* adenylate cyclase fragments T25 and T18. Single colonies were patched onto selective agar containing 100 μg/ml X-Gal and 0.5 mM IPTG. Blue color indicates β-galactosidase activity resulting from interaction between T25 and T18 fusions. A positive control strain expressing T25-zip and T18-zip is shown on the right

3.4 | Spo0J and SMC form a complex in *Staphylococcus aureus* to mediate chromosome segregation

The increased proportion of anucleate cells in the Δ*spo0J* Δ*smc* mutant and the dependence of SMC localization on Spo0J suggested potential interaction between Spo0J and SMC. Therefore, in order to verify whether Spo0J and SMC form a complex in *S. aureus*, we performed co-immunoprecipitation experiments on *S. aureus* RN4220 cells expressing Spo0J-mRFPmars and either GFP or SMC-GFP. Following nuclease digestion of genomic DNA, we used anti-GFP antibodies coupled to magnetic agarose beads to immunoprecipitate GFP or SMC-GFP and their interacting proteins. We were able to detect Spo0J-mRFPmars in the immunoprecipitated complexes isolated from *S. aureus* cells expressing both Spo0J-mRFPmars and SMC-GFP, but not from cells expressing Spo0J-mRFPmars and GFP (Figure 4a). Thus, Spo0J-mRFPmars was isolated specifically in the presence of SMC-GFP, indicating the formation of complexes containing Spo0J and SMC in *S. aureus*. Notably, the Spo0J-mRFPmars immunoprecipitated from cell lysates containing SMC-GFP was only weakly detected using anti-RFP antibodies, which may be indicative of weak or transient complex formation.

To test whether Spo0J and SMC might interact directly, we conducted bacterial two-hybrid assays using Spo0J and SMC fusions to the *Bordetella pertussis* adenylate cyclase (CyaA) fragments, T25 and T18 (Karimova, Pidoux, Ullmann, & Ladant, 1998). The assays revealed that in the *E. coli cya* mutant strain BTH101, β-galactosidase activity was detected from cells expressing the Spo0J-T25 and SMC-T18 fusions (blue patches), however, no activity was detected from cells expressing the reciprocal fusions, SMC-T25 and Spo0J-T18 (white patches) (Figure 4b). We do not exclude the possibility that an interaction between Spo0J and SMC, direct or indirect, may be dependent on Spo0J localization or DNA binding, or on the presence of other *S. aureus* proteins that were not present in the bacterial two-hybrid assays. The assays also showed self-interaction of Spo0J and SMC (Figure 4b), which is consistent with the fluorescent Spo0J-mRFPmars and SMC-GFP foci observed (Figure 3a).

3.5 | Absence of Spo0J and SMC does not interfere with normal *Staphylococcus aureus* cell division

Spatiotemporal coordination of chromosome segregation and cell division is paramount for successful cell growth. Impairment of *parB* in
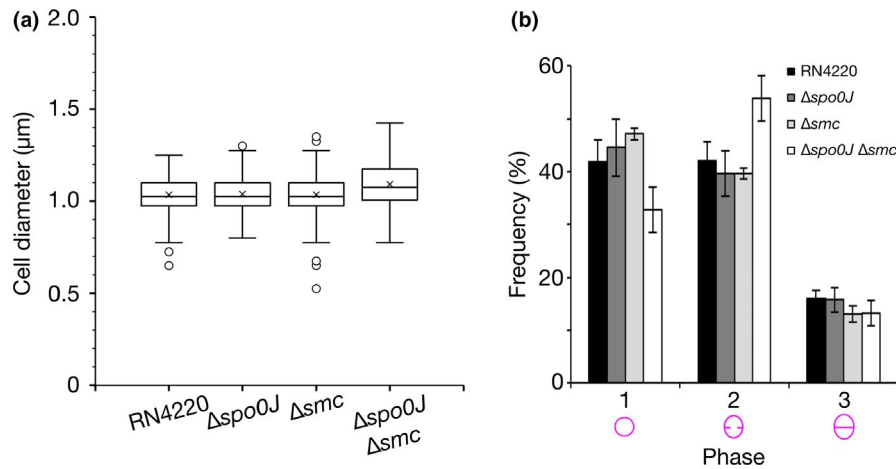
FIGURE 5 (a) Distribution of *Staphylococcus aureus* cell diameters in the presence and absence of *spo0J* and *smc*. Cell diameters were measured from mid-exponential phase *S. aureus* cells grown at 37°C in TSB and stained with the lipid dye FM4-64. Crosses indicate mean; lower, middle, and upper lines of boxes indicate first quartile, median, and third quartile, respectively; ends of whiskers indicate 1.5IQR (interquartile range); circles indicate outliers. n_{total} = 335, 346, 379, and 422 cells for RN4220, Δ*spo0J*, Δ*smc*, and Δ*spo0J* Δ*smc* strains, respectively. No significant difference was detected in cell diameter for Δ*spo0J*, Δ*smc*, and Δ*spo0J* Δ*smc* strains compared to RN4220 (*p* = .7803, 0.9252, and 0.1872, respectively, unpaired Student's *t* test). Histograms showing the distribution of cell diameters are shown in Figure A3. (b) Cell cycle progression of *S. aureus* strains in the presence and absence of *spo0J* and *smc*. Mid-exponential phase *S. aureus* cells were stained with the lipid dye FM4-64, and the frequency of cells in Phase 1 (no septum), Phase 2 (incomplete septum) and Phase 3 (complete septum) of the cell cycle was determined using super-resolution SIM imaging. Graphical representations of the cell cycle phases are shown below the horizontal axis. Data represent averages of three independent experiments. n_{total} = 581, 590, 643, and 646 cells for RN4220, Δ*spo0J*, Δ*smc*, and Δ*spo0J* Δ*smc* strains, respectively. Error bars indicate standard error of the mean

C. crescentus blocks FtsZ ring assembly and subsequent cell division (Mohl et al., 2001), while chromosome segregation defects in *B. subtilis* correlate with elongated cells (Britton et al., 1998; Ireton et al., 1994; Lee & Grossman, 2006). In order to investigate the influence of Spo0J and SMC on *S. aureus* cell division, we sought to determine whether the chromosome segregation defects observed in the *spo0J* and *smc* mutants correspond to abnormalities in staphylococcal cell division.

Disruption of staphylococcal cell division, for example, by impeding FtsZ, EzrA, Noc, or DnaK function, results in cell enlargement and aberrant cell division (Bottomley et al., 2017; Jorge, Hoiczyk, Gomes, & Pinho, 2011; Lund et al., 2018; Monteiro et al., 2018; Pereira et al., 2016; Pinho & Errington, 2003; Veiga et al., 2011). Therefore, as an indicator of cell division, we measured the cell diameters of *S. aureus* cells to determine whether differences in cell size could be attributed to inefficient chromosome segregation. We found no significant difference in cell diameters between the parental and deletion strains (Figure 5a and Figure A3), which suggests that the absence of *spo0J* or *smc*, alone or together, does not affect *S. aureus* cell size.

We next investigated whether *spo0J* and *smc* play a role in cell cycle progression. We categorized the *S. aureus* cell cycle into three phases, characterized by cells that had no septum (Phase 1), an incomplete septum (Phase 2) or a complete septum (Phase 3) (Monteiro et al., 2015). In order to provide an indication of the relative duration of each phase of the cell cycle, we stained *S. aureus* cell membranes with the lipid dye FM4-64 and calculated the proportion of cells in each phase from SIM images. We observed no

difference in the distribution of cells in the three cell cycle phases for the parental, Δ*spo0J*, and Δ*smc* strains (Figure 5b). We did, however, observe a modest, but insignificant, increase in the proportion of cells in Phase 2 for the Δ*spo0J* Δ*smc* double mutant (54 ± 4.3% compared to 42 ± 3.6% for the parental strain, mean ± *SEM*, *p* = .1032) (Figure 5b), potentially indicating slightly prolonged septum closure in these cells. Taken together, these results suggest that *spo0J* and *smc* do not significantly affect cell cycle progression and are not essential for normal cell division in *S. aureus*.

4 | DISCUSSION

In this study, we examined the functional significance of Spo0J and SMC in *S. aureus*, and found that both proteins are required for efficient chromosome segregation, which is consistent with their predicted roles. A single Δ*spo0J* mutant resulted in 0.6% anucleated cells (Figure 2), which is similar to the frequency observed for *B. subtilis* and *S. pneumoniae* mutants (Ireton et al., 1994; Minnen et al., 2011). Our observations for the Δ*smc* mutant are also consistent with the previously shown contribution of SMC to *S. aureus* chromosome segregation (Yu et al., 2010).

Fluorescence localization of Spo0J-mRFPmars and SMC-GFP in *S. aureus* showed that the two proteins formed foci that often overlapped or partially overlapped, and were reminiscent of *oriC* localization (Pinho & Errington, 2004; Veiga et al., 2011) (Figure 3a). Importantly, SMC-GFP localization is dependent on Spo0J, since absence of *spo0J* resulted in a significant reduction in the number

of SMC-GFP foci per cell (Figure 3b–d). This suggests that Spo0J-dependent SMC foci, which likely correspond to complexes containing Spo0J and SMC (Figure 4), are essential for *S. aureus* chromosome segregation. Note that SMC-GFP foci were not completely absent in the Δ*spo0J* mutant, possibly because SMC itself is capable of binding to chromosomal DNA, albeit less efficiently in the absence of ParB/Spo0J (Gruber & Errington, 2009; Minnen et al., 2011; Sullivan et al., 2009). Although our data did not conclusively indicate a direct interaction between Spo0J and SMC, we nonetheless showed that in *S. aureus*, formation of complexes containing Spo0J and SMC is dependent on correct localization of Spo0J (Figure 3b–d). It therefore appears that Spo0J-SMC interaction, direct or indirect, is conserved among several bacterial genera, including *B. subtilis*, *S. pneumoniae*, *C. crescentus*, and *S. aureus* (Gruber & Errington, 2009; Minnen et al., 2011; Sullivan et al., 2009; Tran et al., 2017).

Since *S. aureus* lacks a ParA/Soj ATPase homologue, it is possible that staphylococcal chromosome segregation occurs passively, instead relying on conformational entropy of replicated chromosomes (Jun & Wright, 2010) or on forces generated from cellular processes such as DNA replication or transcription (Dworkin & Losick, 2002; Kjos & Veening, 2014; Lemon & Grossman, 2001). However, interestingly, we found that absence of both *spo0J* and *smc* results in a significantly more severe chromosome segregation defect than absence of either gene alone (Figure 2). This synergistic effect implies that Spo0J and SMC may be partially redundant or offer partial compensation in the absence of the other gene. Furthermore, in light of our finding that accurate chromosome segregation is enhanced by Spo0J in complex with SMC, it is not inconceivable that complexes containing Spo0J and SMC could be involved in additional interactions or processes that are essential for faithful chromosome segregation, such as chromosome organization or compaction. Since a *S. pneumoniae* Δ*parB* Δ*smc* mutant did not show a significant increase in anucleate cells compared to Δ*parB* or Δ*smc* single mutants (Minnen et al., 2011), it would be interesting to investigate whether other, perhaps as yet unknown, proteins or interactions might contribute specifically to chromosome segregation in coccoid-shaped staphylococci. Indeed, the observation that chromosome segregation occurs in the absence of both SMC and a ParA homologue in *S. aureus* suggests that Spo0J facilitates chromosome segregation using a currently unknown mechanism.

A number of bacteria, including *Vibrio cholerae*, *C. crescentus*, and sporulating *B. subtilis*, utilize proteins to anchor chromosomal origins to the cell poles to facilitate chromosome segregation (Ben-Yehuda et al., 2005; Ben-Yehuda, Rudner, & Losick, 2003; Bowman et al., 2008; Ebersbach, Briegel, Jensen, & Jacobs-Wagner, 2008; Yamaichi et al., 2012). Recently, it was shown that *S. aureus* DivIVA, a membrane-localized divisome protein, interacts with SMC, thereby providing a means of coordinating chromosome segregation with cell division, although the exact mechanism is unclear (Bottomley et al., 2017). Accordingly, one could speculate that SMC-DivIVA interaction might act to anchor *oriC*-bound complexes containing Spo0J and SMC during staphylococcal chromosome segregation.

It should be noted that our observations were made on segregation of the bulk chromosome, and as such, we do not exclude the possibility that chromosomal loci might be disorganized or mis-segregated in the absence of either *spo0J* or *smc*. Taking this into account, we did not observe any bisection of the nucleoid by the division septum in any of the strains analyzed. These events were probably prevented by Noc, which prevents divisome assembly over the staphylococcal nucleoid (Veiga et al., 2011), and FtsK and SpoIIIE, which ensure that DNA is not guillotined by the division septum during staphylococcal cell division (Veiga & G Pinho, 2017; Yu et al., 2010). Indeed, an *S. aureus smc spoIIIE* double mutant showed aberrations in chromosome organization and content (Yu et al., 2010). Spo0J and SMC are therefore probably involved in the early stages of *S. aureus* chromosome segregation, immediately following DNA replication, presumably by acting at origin-proximal sites to segregate the origins.

Importantly, although we observed a significant proportion of anucleated cells in the absence of *spo0J* and *smc*, the defect in chromosome segregation was not sufficient to severely affect growth, viability, cell division, or cell cycle progression (Figures 1 and 5). However, it would not be surprising that *S. aureus* utilizes multiple complementary mechanisms, in addition to Spo0J and SMC, to ensure accurate chromosome segregation and coordination with cell division. These additional mechanisms warrant further investigation and may help to better understand how these essential processes are carried out in spherical staphylococci.

CONFLICT OF INTEREST

None declared.

AUTHOR CONTRIBUTION

Helena Chan: Conceptualization; Formal analysis; Investigation; Writing-original draft; Writing-review & editing. Bill Söderström: Supervision; Writing-review & editing. Ulf Skoglund: Supervision; Writing-review & editing.

ETHICS STATEMENT

None required.

DATA AVAILABILITY STATEMENT

Data from this study are available from the corresponding author on reasonable request.

ORCID

Helena Chan https://orcid.org/0000-0002-5194-0006

REFERENCES

Arnaud, M., Chastanet, A., & Débarbouillé, M. (2004). New vector for efficient allelic replacement in naturally nontransformable,

low-GC-content. Gram-positive bacteria. _Applied and Environmental Microbiology_, 70(11), 6887–6891.

Badrinarayanan, A., Le, T. B. K., & Laub, M. T. (2015). Bacterial chromosome organization and segregation. _Annual Review of Cell and Developmental Biology_, 31(1), 171–199.

Baxter, J. C., & Funnell, B. E. (2014). Plasmid partition mechanisms. _Microbiology Spectrum_, 2, 1–20. https://doi.org/10.1128/microbiolspec.PLAS-0023-2014

Ben-Yehuda, S., Fujita, M., Liu, X. S., Gorbatyuk, B., Skoko, D., Yan, J., … Losick, R. (2005). Defining a centromere-like element in _Bacillus subtilis_ by identifying the binding sites for the chromosome-anchoring protein RacA. _Molecular Cell_, 17(6), 773–782.

Ben-Yehuda, S., Rudner, D. Z., & Losick, R. (2003). RacA, a bacterial protein that anchors chromosomes to the cell poles. _Science_, 299(5606), 532–536.

Bloom, K., & Joglekar, A. (2010). Towards building a chromosome segregation machine. _Nature_, 463(7280), 446–456.

Bottomley, A. L., Liew, A. T. F., Kusuma, K. D., Peterson, E., Seidel, L., Foster, S. J., & Harry, E. J. (2017). Coordination of chromosome segregation and cell division in _Staphylococcus aureus_. _Frontiers in Microbiology_, 8, 1–13. https://doi.org/10.3389/fmicb.2017.01575

Bowman, G. R., Comolli, L. R., Zhu, J., Eckart, M., Koenig, M., Downing, K. H., … Shapiro, L. (2008). A polymeric protein anchors the chromosomal origin/ParB complex at a bacterial cell pole. _Cell_, 134(6), 945–955.

Breier, A. M., & Grossman, A. D. (2007). Whole-genome analysis of the chromosome partitioning and sporulation protein Spo0J (ParB) reveals spreading and origin-distal sites on the _Bacillus subtilis_ chromosome. _Molecular Microbiology_, 64(3), 703–718. https://doi.org/10.1111/j.1365-2958.2007.05690.x

Britton, R. A., Lin, D.-C.-H., & Grossman, A. D. (1998). Characterization of a prokaryotic SMC protein involved in chromosome partitioning. _Genes & Development_, 12(9), 1254–1259.

Brzoska, A. J., & Firth, N. (2013). Two-plasmid vector system for independently controlled expression of green and red fluorescent fusion proteins in _Staphylococcus aureus_. _Applied and Environment Microbiology_, 79(9), 3133–3136.

Dworkin, J., & Losick, R. (2002). Does RNA polymerase help drive chromosome segregation in bacteria? _Proceedings of the National Academy of Sciences of the United States of America_, 99(22), 14089–14094.

Ebersbach, G., Briegel, A., Jensen, G. J., & Jacobs-Wagner, C. (2008). A self-associating protein critical for chromosome attachment, division, and polar organization in caulobacter. _Cell_, 134(6), 956–968.

Gerdes, K., Howard, M., & Szardenings, F. (2010). Pushing and pulling in prokaryotic DNA segregation. _Cell_, 141(6), 927–942.

Gibson, D. G., Young, L., Chuang, R.-Y., Venter, J. C., Hutchison Iii, C. A., & Smith, H. O. (2009). Enzymatic assembly of DNA molecules up to several hundred kilobases. _Nature Methods_, 6(5), 343–345.

Graumann, P. L. (2014). Chromosome architecture and segregation in prokaryotic cells. _Journal of Molecular Microbiology and Biotechnology_, 24(5–6), 291–300.

Gruber, S., & Errington, J. (2009). Recruitment of condensin to replication origin regions by ParB/SpoOJ promotes chromosome segregation in _B. subtilis_. _Cell_, 137(4), 685–696.

Gruber, S., Veening, J.-W., Bach, J., Blettinger, M., Bramkamp, M., & Errington, J. (2014). Interlinked sister chromosomes arise in the absence of condensin during fast replication in _B. subtilis_. _Current Biology_, 24(3), 293–298.

Hatano, T., & Niki, H. (2010). Partitioning of P1 plasmids by gradual distribution of the ATPase ParA. _Molecular Microbiology_, 78(5), 1182–1198.

Hayes, F., & Barilla, D. (2006). The bacterial segrosome: A dynamic nucleoprotein machine for DNA trafficking and segregation. _Nature Reviews. Microbiology_, 4(2), 133–143.

Ireton, K., Gunther, N. W., & Grossman, A. D. (1994). _spo0J_ is required for normal chromosome segregation as well as the initiation of sporulation in _Bacillus subtilis_. _Journal of Bacteriology_, 176(17), 5320–5329.

Jensen, R. B., & Shapiro, L. (1999). The _Caulobacter crescentus smc_ gene is required for cell cycle progression and chromosome segregation. _Proceedings of the National Academy of Sciences of the United States of America_, 96(19), 10661–10666.

Jorge, A. M., Hoiczyk, E., Gomes, J. P., & Pinho, M. G. (2011). EzrA contributes to the regulation of cell size in _Staphylococcus aureus_. _PLoS ONE_, 6, https://doi.org/10.1371/journal.pone.0027542

Jun, S., & Wright, A. (2010). Entropy as the driver of chromosome segregation. _Nature Reviews Microbiology_, 8(8), 600–607.

Karimova, G., Pidoux, J., Ullmann, A., & Ladant, D. (1998). A bacterial two-hybrid system based on a reconstituted signal transduction pathway. _Proceedings of the National Academy of Sciences of the United States of America_, 95(10), 5752–5756.

Kjos, M., & Veening, J.-W. (2014). Tracking of chromosome dynamics in live _Streptococcus pneumoniae_ reveals that transcription promotes chromosome segregation. _Molecular Microbiology_, 91(6), 1088–1105.

Kreiswirth, B. N., Lofdahl, S., Betley, M. J., O'Reilly, M., Schlievert, P. M., Bergdoll, M. S., & Novick, R. P. (1983). The toxic shock syndrome exotoxin structural gene is not detectably transmitted by a prophage. _Nature_, 305(5936), 709–712.

Lee, P. S., & Grossman, A. D. (2006). The chromosome partitioning proteins Soj (ParA) and Spo0J (ParB) contribute to accurate chromosome partitioning, separation of replicated sister origins, and regulation of replication initiation in _Bacillus subtilis_. _Molecular Microbiology_, 60(4), 853–869. https://doi.org/10.1111/j.1365-2958.2006.05140.x

Lemon, K. P., & Grossman, A. D. (2001). The extrusion-capture model for chromosome partitioning in bacteria. _Genes & Development_, 15(16), 2031–2041.

Liew, A. T. F., Theis, T., Jensen, S. O., Garcia-Lara, J., Foster, S. J., Firth, N., … Harry, E. J. (2011). A simple plasmid-based system that allows rapid generation of tightly controlled gene expression in _Staphylococcus aureus_. _Microbiology_, 157(3), 666–676.

Lin, D.-C.-H., & Grossman, A. D. (1998). Identification and characterization of a bacterial chromosome partitioning site. _Cell_, 92(5), 675–685.

Livny, J., Yamaichi, Y., & Waldor, M. K. (2007). Distribution of centromere-like _parS_ sites in bacteria: Insights from comparative genomics. _Journal of Bacteriology_, 189(23), 8693–9703.

Löfblom, J., Kronqvist, N., Uhlén, M., Ståhl, S., & Wernérus, H. (2007). Optimization of electroporation-mediated transformation: _Staphylococcus carnosus_ as model organism. _Journal of Applied Microbiology_, 102(3), 736–747.

Lund, V. A., Wacnik, K., Turner, R. D., Cotterell, B. E., Walther, C. G., Fenn, S. J., … Foster, S. J. (2018). Molecular coordination of _Staphylococcus aureus_ cell division. _eLife_, 7, 1–31. https://doi.org/10.7554/eLife.32057

Lutkenhaus, J. (2012). The ParA/MinD family puts things in their place. _Trends in Microbiology_, 20(9), 411–418.

Mascarenhas, J., Soppa, J., Strunnikov, A. V., & Graumann, P. L. (2002). Cell cycle-dependent localization of two novel prokaryotic chromosome segregation and condensation proteins in _Bacillus subtilis_ that interact with SMC protein. _EMBO Journal_, 21(12), 3108–3118. https://doi.org/10.1093/emboj/cdf314

Minnen, A., Attaiech, L., Thon, M., Gruber, S., & Veening, J.-W. (2011). SMC is recruited to _oriC_ by ParB and promotes chromosome segregation in _Streptococcus pneumoniae_. _Molecular Microbiology_, 81(3), 676–688.

Mohl, D. A., Easter, J. Jr, & Gober, J. W. (2001). The chromosome partitioning protein, ParB, is required for cytokinesis in _Caulobacter crescentus_. _Molecular Microbiology_, 42(3), 741–755.

Monk, I. R., Shah, I. M., Xu, M., Tan, M.-W., & Foster, T. J. (2012). Transforming the untransformable: Application of direct

transformation to manipulate genetically *Staphylococcus aureus* and *Staphylococcus epidermidis*. *Mbio*, *3*, 1–11. https://doi.org/10.1128/mBio.00277-11

Monteiro, J. M., Fernandes, P. B., Vaz, F., Pereira, A. R., Tavares, A. C., Ferreira, M. T., … Pinho, M. G. (2015). Cell shape dynamics during the staphylococcal cell cycle. *Nature Communications*, *6*, https://doi.org/10.1038/ncomms9055

Monteiro, J. M., Pereira, A. R., Reichmann, N. T., Saraiva, B. M., Fernandes, P. B., Veiga, H., … Pinho, M. G. (2018). Peptidoglycan synthesis drives an FtsZ-treadmilling-independent step of cytokinesis. *Nature*, *554*(7693), 528–532.

Moriya, S., Tsujikawa, E., Hassan, A. K. M., Asai, K., Kodama, T., & Ogasawara, N. (1998). A *Bacillus subtilis* gene-encoding protein homologous to eukaryotic SMC motor protein is necessary for chromosome partition. *Molecular Microbiology*, *29*(1), 179–187.

Murray, H., Ferreira, H., & Errington, J. (2006). The bacterial chromosome segregation protein Spo0J spreads along DNA from *parS* nucleation sites. *Molecular Microbiology*, *61*(5), 1352–1361.

Oliva, M. A. (2016). Segrosome complex formation during DNA trafficking in bacterial cell division. *Frontiers in Molecular Biosciences*, *3*, 1–9. https://doi.org/10.3389/fmolb.2016.00051

Osorio-Valeriano, M., Altegoer, F., Steinchen, W., Urban, S., Liu, Y., Bange, G., & Thanbichler, M. (2019). ParB-type DNA segregation proteins are CTP-dependent molecular switches. *Cell*, *179*(7), 1512–1524.

Pereira, A. R., Hsin, J., Król, E., Tavares, A. C., Flores, P., Hoiczyk, E., … Pinho, M. G. (2016). FtsZ-dependent elongation of a coccoid bacterium. *Mbio*, *7*, 1–9. https://doi.org/10.1128/mBio.00908-16

Pinho, M. G., & Errington, J. (2003). Dispersed mode of *Staphylococcus aureus* cell wall synthesis in the absence of the division machinery. *Molecular Microbiology*, *50*(3), 871–881.

Pinho, M. G., & Errington, J. (2004). A *divIVA* null mutant of *Staphylococcus aureus* undergoes normal cell division. *FEMS Microbiology Letters*, *240*(2), 145–149.

Pinho, M. G., Kjos, M., & Veening, J. (2013). How to get (a)round: Mechanisms controlling growth and division of coccoid bacteria. *Nature Reviews Microbiology*, *11*(9), 601–614.

Salje, J. (2010). Plasmid segregation: How to survive as an extra piece of DNA. *Critical Reviews in Biochemistry and Molecular Biology*, *45*(4), 296–317.

Sambrook, J., & Russell, D. W. (2001). *Molecular cloning: A laboratory manual*. Cold Spring Harbor, NY: Cold Spring Harbor Laboratory Press.

Sanchez, A., Rech, J., Gasc, C., & Bouet, J. (2013). Insight into centromere-binding properties of ParB proteins: A secondary binding motif is essential for bacterial genome maintenance. *Nucleic Acids Research*, *41*(5), 3094–3103.

Schindelin, J., Arganda-Carreras, I., Frise, E., Kaynig, V., Longair, M., Pietzsch, T., … Cardona, A. (2012). Fiji: An open-source platform for biological-image analysis. *Nature Methods*, *9*(7), 676–682.

Schumacher, M. A. (2012). Bacterial plasmid partition machinery: A minimalist approach to survival. *Current Opinion in Structural Biology*, *22*(1), 72–79.

Soh, Y.-M., Davidson, I. F., Zamuner, S., Basquin, J., Bock, F. P., Taschner, M., … Gruber, S. (2019). Self-organization of *parS* centromeres by the ParB CTP hydrolase. *Science*, *366*(6469), 1129–1133.

Sullivan, N. L., Marquis, K. A., & Rudner, D. Z. (2009). Recruitment of SMC by ParB-*parS* organizes the origin region and promotes efficient chromosome segregation. *Cell*, *137*(4), 697–707.

Toro, E., & Shapiro, L. (2010). Bacterial chromosome organization and segregation. *Cold Spring Harbor Perspectives in Biology*, *2*, a000349. https://doi.org/10.1101/cshperspect.a000349

Tran, N. T., Laub, M. T., & Le, T. B. K. (2017). SMC progressively aligns chromosomal arms in *Caulobacter crescentus* but is antagonized by convergent transcription. *Cell Reports*, *20*(9), 2057–2071.

Tzagoloff, H., & Novick, R. (1977). Geometry of cell division in *Staphylococcus aureus*. *Journal of Bacteriology*, *129*(1), 343–350.

Vecchiarelli, A. G., Hwang, L. C., & Mizuuchi, K. (2013). Cell-free study of F plasmid partition provides evidence for cargo transport by a diffusion-ratchet mechanism. *Proceedings of the National Academy of Sciences of the United States of America*, *110*(15), E1390–E1397.

Vecchiarelli, A. G., Neuman, K. C., & Mizuuchi, K. (2014). A propagating ATPase gradient drives transport of surface-confined cellular cargo. *Proceedings of the National Academy of Sciences of the United States of America*, *111*(13), 4880–4885.

Veiga, H., & G Pinho, M., (2017). *Staphylococcus aureus* requires at least one FtsK/SpoIIIE protein for correct chromosome segregation. *Molecular Microbiology*, *103*(3), 504–517.

Veiga, H., Jorge, A. M., & Pinho, M. G. (2011). Absence of nucleoid occlusion effector Noc impairs formation of orthogonal FtsZ rings during *Staphylococcus aureus* cell division. *Molecular Microbiology*, *80*(5), 1366–1380.

Wang, X., Llopis, P. M., & Rudner, D. Z. (2013). Organization and segregation of bacterial chromosomes. *Nature Reviews Genetics*, *14*(3), 191–203.

Wang, X., Tang, O. W., Riley, E. P., & Rudner, D. Z. (2014). The SMC condensin complex is required for origin segregation in *Bacillus subtilis*. *Current Biology*, *24*(3), 287–292.

Yamaichi, Y., Bruckner, R., Ringgaard, S., Möll, A., Cameron, D. E., Briegel, A., … Waldor, M. K. (2012). A multidomain hub anchors the chromosome segregation and chemotactic machinery to the bacterial pole. *Genes & Development*, *26*(20), 2348–2360.

Yu, W., Herbert, S., Graumann, P. L., & Götz, F. (2010). Contribution of SMC (Structural Maintenance of Chromosomes) and SpoIIIE to chromosome segregation in staphylococci. *Journal of Bacteriology*, *192*(15), 4067–4073.

APPENDIX 1

CONSTRUCTION OF PLASMIDS

pHC052 (P$_{xyl/tetO}$-spo0J-mRFPmars). A 0.85 kb fragment containing *Staphylococcus aureus* RN4220 *spo0J* was PCR-amplified from *S. aureus* genomic DNA using primers spo0J_SalI(F) and spo0J_SacI(R), and then restricted with *Sal*I and *Sac*I. The restricted fragment was purified and ligated with *Sal*I and *Sac*I-digested pSK9065 vector DNA using T4 DNA ligase.

pHC061 (Δspo0J). pHC061 was constructed using Gibson assembly (Gibson et al., 2009). Regions of ~2.5 kb upstream and downstream of *S. aureus* RN4220 *spo0J* were PCR-amplified from *S. aureus* genomic DNA using primer pairs spo0J_up(F)/spo0J_up(R) and spo0J_dwn(F)/spo0J_dwn(R), respectively. pMAD vector DNA was PCR-amplified using primers pMAD_dwn(F) and pMAD_up(R). Amplicons were digested with *Dpn*I to remove methylated template DNA, and then the *spo0J* upstream region, downstream region, and pMAD vector DNA were ligated for 1 hr at 55°C in the presence of 100 mM Tris-HCl (pH 7.5), 10 mM MgCl$_2$, 200 μM of each of the four dNTPs, 10 mM DTT, 5% (w/v) PEG-8000, 1 mM NAD, 3.8 U/ml T5 exonuclease, 23.8 U/ml Q5 DNA polymerase, and 3.8 U/μl Q5 DNA ligase.

pHC067 (P$_{spac}$-smc-gfp). A 3.6 kb fragment containing *S. aureus* RN4220 *smc* was PCR-amplified from *S. aureus* genomic DNA using primers smc_RBS_BamHI(F) and smc_SmaI(R), and then restricted with *Bam*HI and *Sma*I. The restricted fragment was purified and phosphorylated with T4 polynucleotide kinase, then ligated with *Bam*HI and *Sma*I-digested pSK9067 vector DNA using T4 DNA ligase.

pHC080 (Δsmc). pHC080 was constructed using Gibson assembly (Gibson et al., 2009). Regions of ~2.5 kb upstream and downstream of *S. aureus* RN4220 *smc* were PCR-amplified from *S. aureus* genomic DNA using primer pairs smc_up(F)/smc_up(R) and smc_dwn(F)/smc_dwn(R), respectively. The last 0.2 kb at the 3′ end of *smc* was left intact to retain the potential promoter region of a putative downstream gene. pMAD vector DNA was PCR-amplified using primers pMAD_dwn(F) and pMAD_up(R). Amplicons were digested with *Dpn*I to remove methylated template DNA, and then the *smc* upstream region, downstream region, and pMAD vector DNA were ligated for 1 hr at 55°C in the presence of 100 mM Tris-HCl (pH 7.5), 10 mM MgCl$_2$, 200 μM of each of the four dNTPs, 10 mM DTT, 5% (w/v) PEG-8000, 1 mM NAD, 3.8 U/ml T5 exonuclease, 23.8 U/ml Q5 DNA polymerase, and 3.8 U/μl Q5 DNA ligase.

pHC102 (P$_{spac}$-gfp). A 0.7 kb DNA fragment containing *gfp* was amplified from pSK9067 using primers gfp_SalI(F) and gfp_EcoRI(R) and then restricted with *Sal*I and *Eco*RI. The restricted fragment was purified and then ligated with *Sal*I and *Eco*RI-digested pLOW vector DNA (Liew et al., 2011) using T4 DNA ligase.

TABLE A1 Oligonucleotides used in this study

Oligonucleotide	Sequence[a]
gfp_SalI(F)	cgc*gtcgac***aggagg**ataattatttatggtttcaaaaggagaagaac
gfp_EcoRI(R)	cgc*gaattc*ttatttataaagttcgtccataccg
pMAD_dwn(F)	ggatccgatatcgcccgacgcgaggc
pMAD_up(R)	ccatggcatgcatcgatagatctgtc
smc_BamHI(F)	cgc*ggatcc*atggtttatttaaaatcaatag
smc_KpnI(R)	cgc*ggtacc*gcttgctcctccttcaacacatc
smc_RBS_BamHI(F)	cgc*ggatcc***aggagg**ataattattatgtggtttatttaaaatcaatag
smc_dwn(F)	ctttaaaattgtgataaggagtttaggatggatgaggttgaagctgcactag
smc_dwn(R)	tccagcctcgcgtcgggcgatatcggatcccataaactgcttgtctactcac
smc_SmaI(R)	gcg*cccggg*accagctgatgcagcagaacctcc*ttgctcctccttcaacacatc
smc_up(F)	actagacagatctatcgatgcatgccatggcagtagcgttcttagcatcag
smc_up(R)	tgcttcatctagtgcagcttcaacctcatccatcctaaactccttatcac
spo0J_BamHI(F)	cgc*ggatcc*atgagtgaattgtcaaaaag
spo0J_SacI(R)	cgc*gagctc*gctttaccatacctacgatttaattg
spo0J_dwn(F)	aactgttataagatattaattagcttacagaggtatggtaaatagttaca
spo0J_dwn(R)	tccagcctcgcgtcgggcgatatcggatccgcacctttcacaataccagc
spo0J_SacI(R)	gcg*gagctc**ggaggcgccgcagga*tttaccatacctacgatttaattg
spo0J_SalI(F)	cgc*gtcgac***aggagg**ataattatttgtgagtgaattgtcaaaaagtg
spo0J_up(F)	actagacagatctatcgatgcatgccatgggtttgcccgctatatagtac
spo0J_up(R)	atataaaattgtgtaactatttaccatacctgtaagctaattaatatcttataacag

[a]Oligonucleotides are presented 5′–3′, left to right. Restriction sites are underlined. Ribosome binding sites are highlighted in bold. Linker sequences are italicized.
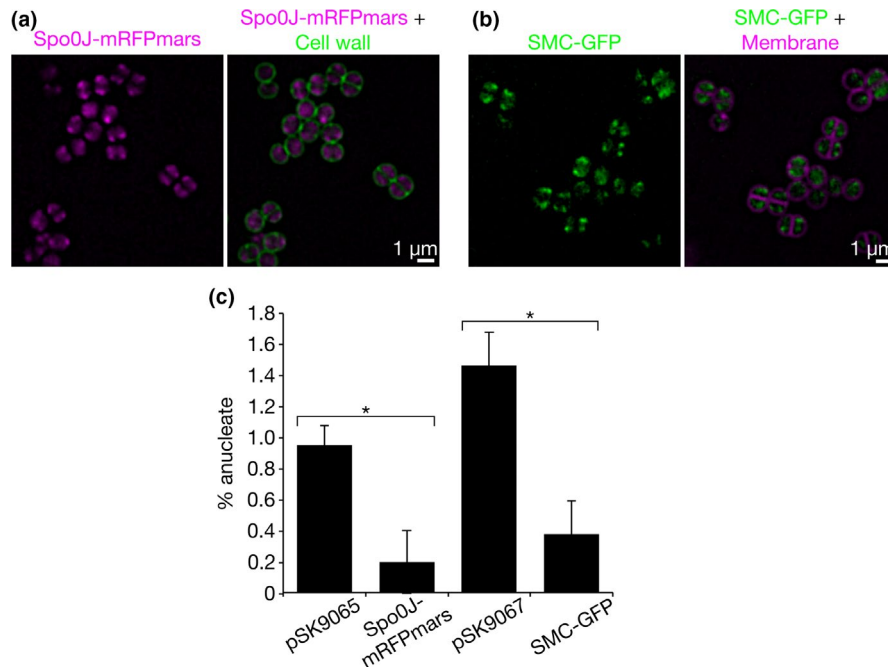
FIGURE A1 Complementation of _Staphylococcus aureus_ Δspo0J and Δsmc strains. (a) SIM images of Spo0J-mRFPmars in _S. aureus_ Δspo0J. Cell walls were labelled with a vancomycin BODIPY FL conjugate. (b) SIM images of SMC-GFP in _S. aureus_ Δsmc. Cell membranes were labelled with FM4-64. Scale bars = 1 μm. (c) Frequency of anucleate cells in _S. aureus_ Δspo0J cells carrying mRFPmars empty vector (pSK9065) or pHC052 (Spo0J-mRFPmars) and in _S. aureus_ Δsmc cells carrying GFP empty vector (pSK9067) or pHC067 (SMC-GFP). Cells were grown at 37°C with 2.5 ng/ml anhydrotetracycline or 0.1 mM IPTG for Δspo0J and Δsmc strains, respectively. Data represent averages of three independent experiments. n_{total} = 1,268, 1,264, 1,638, and 931 cells for pSK9065, Spo0J-mRFPmars, pSK9067, and SMC-GFP strains, respectively. Error bars indicate standard error of the mean. *p < .05, considered statistically significant (unpaired Student's _t_ test)
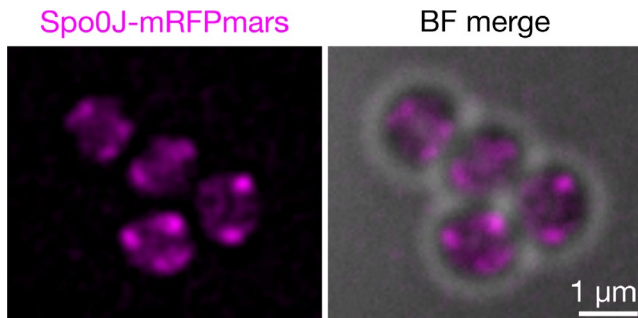

FIGURE A2 SIM image of Spo0J-mRFPmars (magenta) in _Staphylococcus aureus_ RN4220 cells induced with 2.5 ng/ml anhydrotetracycline. Merge with brightfield image is shown on the right. Scale bar = 1 μm

pHC111 (spo0J-T25) and pHC114 (spo0J-T18). A 0.85 kb DNA fragment containing _S. aureus spo0J_ was amplified from _S. aureus_ RN4220 genomic DNA using primers spo0J_BamHI(F) and spo0J_SacI(R) and then restricted with _Bam_HI and _Sac_I. The restricted fragment was purified and then ligated with _Bam_HI and _Sac_I-digested pKNT25 or pUT18 vector DNA using T4 DNA ligase.

pHC112 (smc-T25) and pHC115 (smc-T18). A 3.6 kb DNA fragment containing _S. aureus smc_ was amplified from _S. aureus_ RN4220 genomic DNA using primers smc_BamHI(F) and smc_KpnI(R) and then restricted with _Bam_HI and _Kpn_I. The restricted fragment was purified and then ligated with _Bam_HI and _Kpn_I-digested pKNT25 or pUT18 vector DNA using T4 DNA ligase.
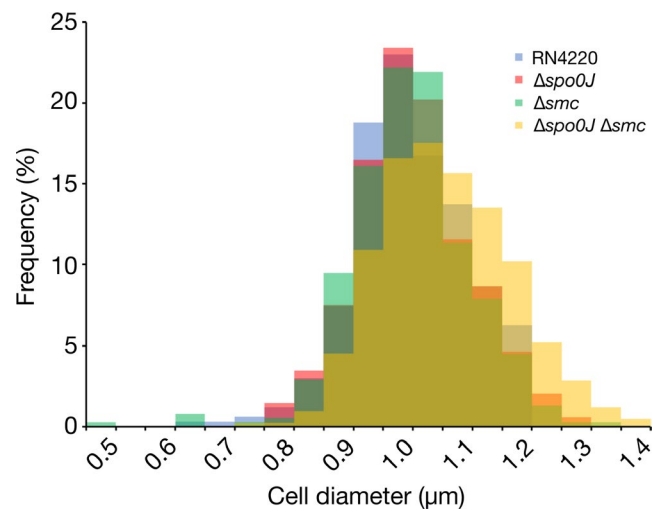

FIGURE A3 Histogram of cell diameters for _Staphylococcus aureus_ RN4220 (blue), Δspo0J (red), Δsmc (green), and Δspo0J Δsmc (yellow). Cell diameters were measured from mid-exponential phase _S. aureus_ cells grown at 37°C in TSB and stained with the lipid dye FM4-64

CONSTRUCTION OF _STAPHYLOCOCCUS AUREUS_ DELETION STRAINS

Electrocompetent _S. aureus_ RN4220 cells were electroporated with the integration plasmid pHC061 or pHC080 to generate _spo0J_

(HC061) and _smc_ (HC080) deletions, respectively. Electroporated cells were incubated at 30°C on BHI agar containing 10 μg/ml of erythromycin and 100 μg/ml of 5-bromo-4-chloro-3-indolyl-β-D-galactopyranoside (X-Gal) (BHI/Em/X-Gal) to select for transformants. Blue colonies were grown in TSB containing 10 μg/ml of erythromycin at 43°C for ~8 hr, and then streaked on BHI/Em/X-Gal agar. Plates were incubated at 43°C to promote vector integration into the chromosome via homologous recombination. Single blue colonies were selected and continuously subcultured approximately six times at 30°C in TSB without antibiotic selection to promote double cross-over and plasmid loss. The final subculture was serially diluted in PBS, spread on BHI/X-Gal agar plates, and incubated at 30°C. Single colonies were replica-patched onto BHI/X-Gal agar plates with and without erythromycin selection. White patches that were erythromycin-resistant, indicating plasmid excision from the chromosome, were selected and screened for gene deletion. Gene deletions were verified by PCR of isolated genomic DNA.

The _S. aureus_ Δ_spo0J_ Δ_smc_ double mutant (HC094) was generated in HC061 (Δ_spo0J_) using the integrative plasmid, pHC080, to generate an additional _smc_ deletion as described above.